Preprints of the 21st IFAC World Congress (Virtual)
Berlin, Germany, July 12-17, 2020

Multi-objective trajectory design for overtaking maneuvers of automated vehicles

Tamás Hegedűs *, **Balázs Németh** **, **Péter Gáspár** **

* *Department of Control for Transportation and Vehicle Systems, Budapest University of Technology and Economics, Stoczek u. 2, H-1111 Budapest, Hungary. E-mail: hegedus.tamas@mail.bme.hu*
** *Systems and Control Laboratory, Institute for Computer Science and Control, Kende u. 13-17, H-1111 Budapest, Hungary. E-mail: [balazs.nemeth;peter.gaspar]@sztaki.hu*

Abstract: The paper proposes a trajectory design method for overtaking maneuvers, in which several performances are incorporated. Thus, it leads to a multi-objective optimization task. It is based on a simple mathematical representation of feasible trajectories by using a potential field approach. The solution of the complex computations in the optimization is approximated by neural networks. The proposed solution is based on the idea that there are a large number of collision free feasible trajectories. The goal of the method is to find the trajectory, which is suitable for the specified objectives. The result of the paper is an integrated decision for both longitudinal and lateral directions, such as longitudinal acceleration command and the values of the defined path. The effectiveness of the method is presented through CarMaker simulation environment.

Keywords: automated vehicles, overtaking strategy, potential field, neural network,

1. INTRODUCTION AND MOTIVATION

The development of automation in overtaking maneuvers can contribute to the avoidance of emergency in traffic scenarios. Through the automation the elimination of accident caused by the human errors can be achieved. Moreover, the trajectory of the overtaking maneuver must be carefully selected, considering the human requirements, the traffic environment and the dynamical properties of the automated vehicle.

In the field of overtaking control of autonomous vehicles several different approaches have been developed. The advantage of the Model Predictive Control (MPC)-based approaches is that they consider the prediction about the surrounding vehicles in the design of the current intervention. For example, in Berntorp [2017] a technique for path planning together with collision avoidance with the application of overtaking was found. Moreover, in the method the surrounding vehicles were considered through stochastic approaches. However, a drawback of the MPC-based methods can be their high computation requirements, which motivates the application of further control methods. In the work of Karlsson et al. [2019] a computationally efficient modeling approach for the challenges of overtaking maneuvers was developed. Another mixed integer programming method, in which the complexity of the computation and the number of variables were reduced, was proposed by Molinari et al. [2017]. In another method proposed by Nguyen et al. [2017] the overtaking task was solved through a stochastic predictive control method while the longitudinal and lateral velocities of the surrounding vehicles were predicted. In You et al. [2019] Bézier curves for trajectory planning were used. In Zhang et al. [2018] a decision making was proposed by using reinforcement learning frameworks to obtain overtaking maneuvers. In Petrov and Nashahibi [2014] a nonlinear adaptive controller for a two-vehicle automated overtaking maneuver as a tracking task was presented.

The contribution of this paper is a trajectory design method for overtaking maneuver, in which several objectives can be incorporated. It is achieved by two ways: first, all of the feasible trajectories are represented by a distinct potential value, which induces a simplified search algorithm in the optimization process. Second, the solution

[1] The research was supported by the Hungarian Government and cofinanced by the European Social Fund through the project "Talent management in autonomous vehicle control technologies" (EFOP-3.6.3-VEKOP- 16-2017-00001).
The research reported in this paper was supported by the Higher Education Excellence Program of the Ministry of Human Capacities in the frame of Artificial Intelligence research area of Budapest University of Technology and Economics (BME FIKPMI/FM).
The work of Balázs Németh was partially supported by the János Bolyai Research Scholarship of the Hungarian Academy of Sciences and the ÚNKP-19-4 New National Excellence Program of the Ministry for Innovation and Technology.
The work of Tamás Hegedűs was partially supported by the ÚNKP-19-3 New National Excellence Program of the Ministry for Innovation and Technology.

of the complex computations is approximated by neural networks. The goal of the method is to find a collision-free trajectory, which is also suitable for the appropriate performance specifications.

The structure of the paper is the following. Section 2 presents the formulation of the feasible trajectories. Section 3 introduces the potential field functions for various performances. The optimization task of the trajectory design and the machine-learning based training process are proposed in Section 4. The algorithm is illustrated through simulation examples in Section 5. Finally, in Section 6 the contributions of the paper are concluded.

2. FORMULATION OF TRAJECTORY SCENARIOS FOR OVERTAKING

The purpose of this section is to determine the set of feasible overtaking trajectories, which is the basis of the selections of the appropriate trajectory.

The trajectory of the overtaking maneuver is formed as a piecewise-clothoid function, which contains four clothoid segments, which are connected to each other. The trajectory is depicted by three main parameters, such as the start and final longitudinal positions x_s, x_f of the overtaking section and the final lateral position of the end of the curve y. Different lateral displacements are taken into account to provide a general model for path planning (e.g. overtaking a bicycle or a truck). The start of the curve is determined by x_s and the current lateral position of the vehicle y_v, while end of the curve is described by the pair x_f, y.

The advantage of the piecewise-clothoid formulation is that it guarantees a continuous, smooth and bounded trajectory. The points of the trajectory can be computed through the general form (Gray [1993]) as

$$x(s) = a\sqrt{\pi}S\left(\frac{s}{\sqrt{\pi}}\right), \tag{1a}$$

$$y(s) = a\sqrt{\pi}C\left(\frac{s}{\sqrt{\pi}}\right), \tag{1b}$$

where $S(\cdot)$ and $C(\cdot)$ are Fresnel sine and cosine, a is a scaling factor and s represents arc value during the clothoid. The trajectory is computed based on (1) between the start point with x_s, y_v and the end point x_f, y. The final trajectory is built up with 4 segments, in which the parameter of the clothoid sharpness α is selected for the same. It results in that the overtaking trajectories are symmetrical on their center. Thus, the value of the trajectory curvature κ is computed as

$$\kappa = s\alpha. \tag{2}$$

Due to comfort requirements the gradient of the line between the start and the end points must be limited. The maximum gradient is determined by the requested maximum lateral acceleration of the vehicle, which is computed as

$$a_{lat,max} \geq v_{long}^2 \kappa_{max}, \tag{3}$$

where κ_{max} is the maximum curvature of the clothoid and v_{long} is the actual velocity. Using κ_{max}, (1) and (2) the maximum value of the gradient can be calculated. Due to the Fresnel sine and cosine expressions in (1) the computation can be performed via a recursive method. The value of $a_{lat,max}$ is selected based on the suggestions of empirical studies, e.g. Xu et al. [2015] defines the comfortable value on the lateral acceleration as $a_{lat,max,1} = 1.8m/s^2$, a medium comfort value as $a_{lat,max,2} = 3.6m/s^2$, while $a_{lat,max,3} = 5m/s^2$ is the maximum for extreme scenarios.

The set of candidate start and end points for the selection of the feasible trajectories depicts a parallelogram, as it is illustrated in Figure 1. The parallelogram is gridded in longitudinal and lateral directions with n and m equidistant segments. Through the increase in the number of the grid points the number of the feasible trajectories increases dramatically, for example the selection of $n = m = 3$ results in 18 trajectories, while $n = m = 4$ or $n = m = 5$ leads to 40 and 75 trajectories, as presented below. Thus, it is recommended to minimize the size of the grid. The maximum horizon of x_s and x_f must be selected to avoid the insufficiently high time requirement of the overtaking maneuver.

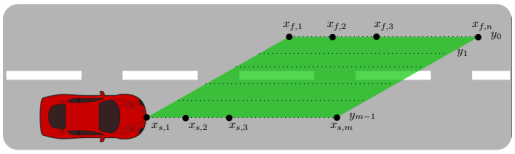

Fig. 1. Candidate start and end points of the trajectories

The set of feasible trajectories are determined by the candidate start and end points. Due to the acceleration constraint (3) the requirement against the feasible trajectories is

$$i \leq j \quad \forall\, x_{s,i}, x_{f,j}, \qquad i \in [1; m],\ j \in [1; n]. \tag{4}$$

Using the criteria (4) an adjacency matrix χ_0 between the candidate start and end points is formed as

$$\chi_0 = \begin{bmatrix} x_{s,1}, x_{f,1}, y_1 & x_{s,1}, x_{f,2}, y_1 & \dots & x_{s,1}, x_{f,n}, y_1 \\ x_{s,1}, x_{f,1}, y_2 & x_{s,2}, x_{f,2}, y_1 & \dots & x_{s,2}, x_{f,n}, y_1 \\ x_{s,1}, x_{f,1}, y_3 & x_{s,2}, x_{f,2}, y_2 & \dots & x_{s,3}, x_{f,n}, y_1 \\ \vdots & \vdots & \ddots & \vdots \\ x_{s,1}, x_{f,1}, y_m & x_{s,3}, x_{f,2}, y_{m-1} & \dots & x_{s,m}, x_{f,n}, y_1 \end{bmatrix}, \tag{5}$$

which contains the feasible trajectories. For example, the trajectory $x_{s,i}, x_{f,j}, y_0$ represents that the vehicle changes the lane, $x_{s,i}, x_{f,j}, y_{m-1}$ represents pure straight motion while the further trajectories represent a lateral motion with slight lateral displacement. χ_0 has the size $m\sum_{i=1}^{n} i$ due to the constraint (4).

In general case, the road can have more than 2 lanes, which induces that the set of feasible trajectories is increased. Considering that the overtaking maneuver is designed for the change of only one lane, the adjacency matrix is extended for left and right lane directions. Thus, the general adjacency matrix χ is resulted as the extension

$$\chi = \begin{bmatrix} \chi_0|_{(x_{s,i}, x_{f,j}, y_k} \\ \chi_0|_{x_{s,i}, x_{f,j}, -y_k} \end{bmatrix}, \tag{6}$$

where $k \in [0; m-1]$ and χ has the size $2 \cdot m\sum_{i=1}^{n} i$.

Figure 1 illustrates an example on the feasible trajectories for a 2 lane scenario with $n = 4$, $m = 3$ and the considered

maximum acceleration is $a_{lat,max} = 3.6m/s^2$. The resulted adjacency matrix χ has the size $3 \cdot (1+2+3+4)$, which results in 30 distinct trajectories.

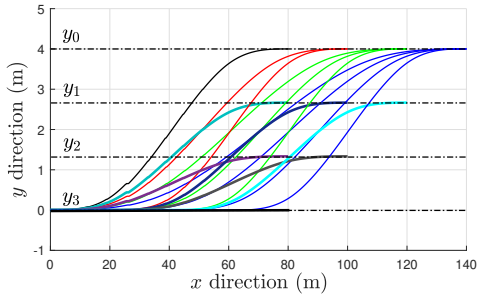

Fig. 2. Illustration of the feasible trajectories

3. PERFORMANCE REQUIREMENTS AGAINST THE OVERTAKING TRAJECTORY

The trajectory of the overtaking maneuver must guarantee several performances, which are posed by the safety and comfort requirements. In this section these performances are defined, such as the requirement on the lateral acceleration, the consideration of the surrounding vehicles, the avoidance of the lane departure and the holding of the safe vehicle inter-distance. These performances describe potential fields, which are taken parts in the trajectory optimization process (see e.g. Switkes et al. [2004]).

3.1 Requirement on traveling comfort

An important component of the traveling comfort in overtaking maneuvers is the lateral acceleration, which must be minimized. Although in the determination of the feasible sets $a_{lat,max}$ has already been considered (see (3)), it is also necessary to minimize the value of a_{lat}. It motivates that the handling of lateral acceleration must be incorporated in the performance requirements. The lateral acceleration can be computed along the feasible trajectories. For a given $j \in \left[1; 2 \cdot m \sum_{i=1}^{n} i\right]$ trajectory the maximum acceleration is computed as

$$a_{lat,j}(s) = v_{long}^2 \kappa(s), \tag{7a}$$

$$a_{lat,j,max} = \max\left(a_{lat,j}(0) \dots a_{lat,j}(L)\right), \tag{7b}$$

where L is the length of the trajectory and κ is resulted by the clothoid curves of trajectory j, see Section 2. Thus, every feasible trajectory of χ is represented by a value $a_{lat,j,max}$.

The performance of the traveling comfort is represented by a potential field, whose discrete function $P_a(j)$ is characterized by $a_{lat,j,max}$ for all trajectories. The following sigmoid function, which is commonly used in autonomous decision making process (see e.g. Wissing et al. [2017]), weights the trajectories according to their maximal lateral acceleration values

$$P_a(j) = \frac{2}{1 + e^{-\xi \cdot a_{lat,j,max}}} - 1, \tag{8}$$

where the value of ξ is a tuning defined parameter.

3.2 Avoidance of the surrounding vehicles

An important safety performance is to guarantee the avoidance of the surrounding vehicles during the motion of the automated vehicle. For this purpose a potential function is used, which has longitudinal and lateral components. The potential field describes the probability of the collision based on the predicted motions of the vehicles. It is considered that there are N number of vehicles in the surrounding of the automated (ego) vehicle, which are indexed with k. All of the vehicles is characterized by a potential field function P_k with longitudinal and lateral components.

The values of the potential field functions are computed for discrete points around the neighborhood of a given trajectory, where ego vehicle can have position. An illustrative example is found in Figure 3.

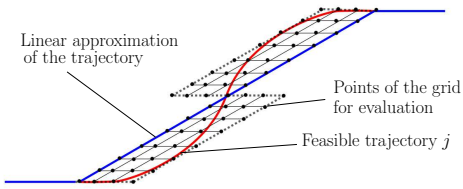

Fig. 3. Evaluation of the trajectory j for vehicle k

First, the longitudinal component of the potential field function is formed. During the prediction it is assumed that vehicle k has a constant velocity, while ego vehicle has a constant acceleration on the prediction horizon. Its reason is that the measurement of the acceleration of vehicle k can be difficult, while the actual velocity can be estimated through the sensors of the automated vehicle. The longitudinal velocity of vehicle k is v_k and the inter-distance between the vehicles is d_k.

The formulation of the potential field function is based on the idea that the change of the inter-distance on the predicted horizon is examined. During the analysis the inter-distance is transformed to an equivalent time value Δt_i. It expresses that ego vehicle can reach vehicle k during Δt_i, which is equivalent to the reduction of the inter-distance to zero. The advantage of this approach is that it contains the velocity and the inter-distance information jointly about the vehicles, which makes the formulation less complex.

The actual inter-distance d_k between the vehicles is divided into l number of equidistant segments, such as $0 \dots \frac{i \cdot d_k}{l} \dots d_k$, where index i is between 0 and l. Distance $\frac{i \cdot d_k}{l}$ is performed by vehicle k during the time $\frac{i \cdot d_k}{l v_{long}}$. During the same time value, the inter-distance is predicted to

$$\Delta s_i = v_k \frac{i \cdot d_k}{l v_{long}} - \frac{1}{2} a_{long} \left(\frac{i \cdot d_k}{l v_{long}}\right)^2 + d_k - \frac{i \cdot d_k}{l} \tag{9}$$

The inter-distance Δs_i is transformed to time value Δt_i based on the kinematic motion equations of the vehicle. Considering the constant velocity for vehicle k and constant acceleration for the ego vehicle the equivalent time to reduce Δs_i to zero is

$$\Delta t_i = \frac{-(v_{long} - v_k) + \sqrt{(v_{long} - v_k)^2 + 2a_{long}\Delta s_i}}{a_{long}}. \tag{10}$$

The potential field function of vehicle k in longitudinal direction for $\Delta t_{j,i}$ is defined by exponential function (Rasekhipour et al. [2017]), such as

$$P_{long,k,j}(\Delta t_i) = \min\left(b\zeta(1 - \zeta^{\frac{1}{\Delta t_{j,i}}}), 1\right), \tag{11}$$

where b and ζ are design parameters. The value of the potential function for a trajectory j is represented by a discrete value, which is limited to 1 due to normalization reasons. Second, it is necessary to calculate the function of the potential field in lateral direction. An applicable form of the Gaussian function is used by Papoulis [1965], where the expected value of the distribution function for a given surrounding vehicle is

$$P_{lat,k,j}(y) = \frac{1}{\sigma\sqrt{2\pi}} e^{\frac{(y-c)^2}{2\sigma^2}}, \tag{12}$$

where c is a parameter and the standard deviation can be computed using the width of the vehicle y_v, such as $\sigma = \frac{\sqrt{y_v}}{4}$. The value of $P_{lat}(y)$ is in a normalized form.

The potential field function for vehicle k is resulted by the multiplication of $P_{long,k,j}$ and $P_{lat,k,j,i}$ (see (11) and (12)). The values of the potential field function for vehicle k and trajectory j in a given point i, y is computed as

$$P_{k,j}(\Delta t_i, y) = P_{long,k,j}(\Delta t_i) P_{lat,k,j}(y). \tag{13}$$

The result of the computation is the maximum value of $P_{k,j}(\Delta t_i, y)$ for all $\Delta t_i, y$ pairs on the grid of Figure 3, such as

$$P_{k,j} = \max(P_{k,j}(\Delta t_1, -y_v) \dots \Delta t_z, y_v)). \tag{14}$$

Figure 4 shows an example of the potential field function. Vehicle k is in front of the ego vehicle with $\zeta = 0$ and $y_v = 2m$ settings. The time difference between the two vehicles varies between $1s$ and $0s$.

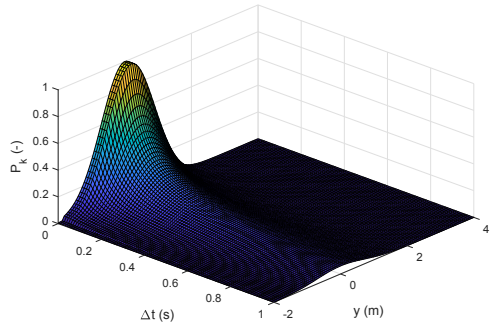

Fig. 4. Example on the function of the potential field for the motion of a surrounding vehicle

3.3 Avoidance of the lane departure

During the motion of the vehicle it is necessary to guarantee that the vehicle has a safe distance from the edge of the road. Moreover, under normal circumstances the straight motion of the vehicle is requested in the center of the lane. The role of the potential field P_{lane} is to focus on these performance requirements. In Rasekhipour et al. [2017] a quadratic function is recommended as a potential field. In this paper it is extended on a way to consider at least two lanes on the road, which leads to the nonlinear function

$$P_w(y, W_r) = (\frac{y^2 + 1}{W_r^2} + 0.1)(\cos(\frac{y\pi}{0.5W_r}) + 1), \tag{15}$$

where W_r is the width of one lane. The presented formula guarantees that the potential field function has minimum in the center of the lanes. P_w value is normalized to eliminate the impact of W_r such as

$$P_{lane}(y) = \frac{P_w(y, W_r)}{P_w(y, 0.5W_r)}. \tag{16}$$

3.4 Tracking the reference velocity

Finally, the impact of the longitudinal decision making is incorporated in the performance of the velocity tracking. The reference velocity on the given road segment is defined as v_{ref}. Since the motion of ego vehicle is considered to have constant acceleration, the velocity of the vehicle $v_{long,L}$ at the end of the prediction horizon L can computed through the kinematic relations. The function of the potential field penalizes the difference between the reference velocity and the predicted velocity as

$$P_v(a_{long}) = \min\left(\frac{|v_{ref} - v_{long,L}(a_{long})|}{\epsilon}, 1\right), \tag{17}$$

where ϵ is a normalizing factor, which represents a maximum difference between the velocities. The function is limited to 1 for the comparison with the further potential field functions.

4. DESIGN OF MULTI-OBJECTIVE TRAJECTORY

The design of the vehicle trajectory is computed based on the potential fields, which are related to each performances. The selection of the trajectory is based on a multi-objective optimization problem, whose cost function contains the weighted sum of the potential field functions. In this section the optimization problem and its solution are proposed. The cost function of the optimization is formed as

$$P(x_s, x_f, y, a_{long}) = q_1 P_a(j(x_s, x_f, y)) + \\ + q_2 \sum_{k=1}^{N} P_{k,j}(x_s, x_f, y, a_{long}) + q_3 P_{lane}(y) + q_4 P_v(a_{long}), \tag{18}$$

where q_1, q_2, q_3 and q_4 are design parameters to guarantee the priorities between the performances. Since, the potential fields are normalized to 1, the tuning parameters help to give more attention to safety.

The optimization problem based on (18) is formed as

$$\min_{x_s, x_f, y, a_{long}} P(x_s, x_f, y, a_{long}) \tag{19a}$$

subject to

$$(x_s, x_f, y) \in \chi, \tag{19b}$$

which means that x_s, x_f, y triad must be selected from the set of feasible trajectories. The calculation of P in the discrete points around the trajectories requires only operations with low computational complexity.However,

the online solution of the problem (19) can require lots of time if the number of the surrounding vehicles or the size of χ are increased.

The reduction of the computation time is achieved through the application of machine-learning. Through the method a neural network is generated, whose role is to learn the cost function P for various vehicle dynamic scenarios. For the determination of the number of neurons and hidden layers the so-called k-fold cross validation method can be used. The training process of the neural network is based on samples, whose set is divided into two subsets: the role of the training set is to train the neural network, while test set is for validation purposes. In this case, the rectified linear unit (ReLU) and the log-sigmoid functions are used as an activation function. 5The trained neural network consists of 4 hidden layers, which consists of 20-25-30-20 neurons. In the training process the Levenberg-Marquardt algorithm is used, see M. Hagan and Beale [1996].
Data set for training and test purposes is generated over 5000 different scenarios, where the following parameters are varied randomly:

- actual and reference velocity of ego vehicle,
- lateral position, acceleration of the ego vehicle,
- velocities and inter-distances related to the surrounding vehicles,
- lateral positions and width values of the surrounding vehicles.

The prediction horizon is divided into $n = m = 6$ segments. Using these inputs the potential field functions are computed and saved. Neural network is trained with different parameters, as it is presented in 4, where FR and FL represent the front right and front left vehicle, d the distance from the given vehicle and v is the velocity and the lateral positions (y) and the width of the obstacles (w) are also given.

Parameters	Case 1
v_{long}, v_{ref} (m/s)	30.4, 29
y (m), a_{long} (m/s^2)	0, -1.15
d_{FR} (m), v_{FR} (m/s)	50, 26.6
y_{FR}, w_{FR} (m)	-0.6, 1.7
d_{FL} (m), v_{FL} (m/s)	21.8, 15.6
y_{FL}, w_{FL} (m)	4.4, 0.75

Table 1. Parameters of the test scenarios

In Figure 5 the result of the neural network can be compared to the previously computed potential field of the algorithm. The minimum value of the surface is at the sixth row and at the first column. According to the definition of χ matrix, the ego vehicle do not start overtaking, because the preceding vehicle is far from it.

5. SIMULATION EXAMPLE

The effectiveness of the presented algorithm is illustrated through two examples, which have been simulated in CarMaker vehicle dynamics simulation software. During the simulation the tracking of the calculated route and velocity profile have been tracked through the built-in automated PID-based driver models. The control inputs are the steering angle and the pedal position.

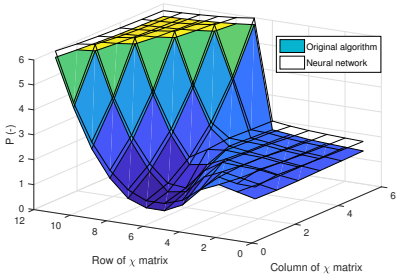

Fig. 5. Result of case 1

5.1 Longitudinal approaching scenario

In this scenario the effectiveness of the method is illustrated, when the overtaking is not possible. It results in that the preceding vehicle must be followed after an approaching maneuver. During the simulation it is necessary to make decision in longitudinal direction, in order to avoid the collision, when the situation cannot be solved by only a lateral control. Since the overtaking is not executable, the vehicle starts decreasing its velocity, see Figure 6(a). The difference between the two vehicles are $15m$, which satisfy the predefined safety requirements, see Figure 6(b).

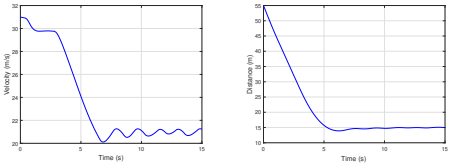

(a) Velocity (b) Distance from the vehicle

Fig. 6. Results of the longitudinal approaching scenario

5.2 Complex overtaking scenario

In Figure 7 a complex overtaking scenario is presented, in which there are two surrounding vehicles.

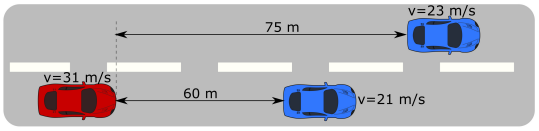

Fig. 7. Simulation example scenario

The initial velocity of the ego vehicle is set to $31m/s$ and the reference velocity is selected to $v_{ref} = 30m/s$. Figure 8 shows the steering input, the velocity and the lateral position of the vehicle in the given scenario. The velocity of the vehicle during the simulation is presented in Figure 8(c). As an important performance, the lateral acceleration of the vehicle is illustrated in Figure 8(d). It can be seen that the acceleration value is inside of the comfortable range $\pm 1.8m/s^2$.

The various sections of the overtaking maneuver are illustrated in Figure 9. On the left side of the illustration the given situation can be seen, while on the right side the actual potential field, which is computed by the proposed algorithm.

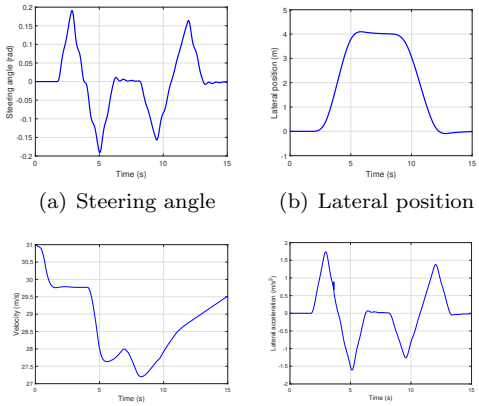

(a) Steering angle (b) Lateral position

(c) Velocity of the vehicle (d) Lateral acceleration

Fig. 8. Results of the complex scenario

Figure 9(a) shows the scenario ($t = 1.5$) before the overtaking has been started. The surrounding vehicles are far from the ego vehicle, which means that P_{lane} has the highest impact on P. Due to the shape of P the straight motion is preferred. There are high values in the upper triangle of the matrix, because the final positions of that trajectories are outside the road, which must be avoided. In Figure 9(b) ($t = 3.6s$) the start of the overtaking maneuver is shown. In the function of P the surrounding vehicles have high impact via P_k and the lateral motion is started. Finally, in Figure 9(d) at ($t = 10.6s$) the end of the overtaking maneuver can be seen, and the minimum of the function represents the returning maneuver to the right lane.

6. CONCLUSIONS

The results of the method illustrated that the automated vehicle with the proposed trajectory design method is able to handle the motion of surrounding vehicles in longitudinal and lateral directions. The simulations presented that the selected trajectory is comfortable with smooth profile and low lateral acceleration, while the collision with the surrounding vehicles is avoided. The proposed solution can be a promising method for the control strategy of the automated vehicles in the layer of the trajectory design.

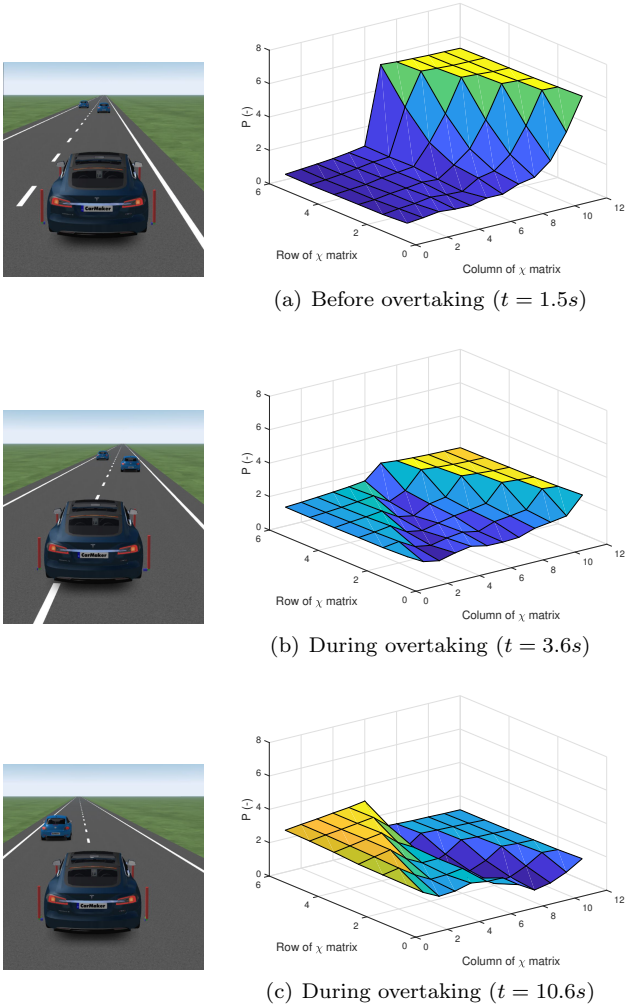

(a) Before overtaking ($t = 1.5s$)

(b) During overtaking ($t = 3.6s$)

(c) During overtaking ($t = 10.6s$)

Fig. 9. Illustration of the complex maneuver

REFERENCES

K. Berntorp. Path planning and integrated collision avoidance for autonomous vehicles. In *American Control Conference*, pages 4023–4028, May 2017.

Alfred Gray. *Modern Differential Geometry of Curves and Surfaces*. CRC Press, 1993.

Johan Karlsson, Nikolce Murgovski, and J. Sjöberg. Computationally efficient autonomous overtaking on highways. *IEEE Transactions on Intelligent Transportation Systems (Early Access)*, 2019.

H. Demuth M. Hagan and M. Beale. *Neural Network Design*. Boston: PWS Publishing, 1996.

F. Molinari, Nguyen Ngoc Anh, and L. Del Re. Efficient mixed integer programming for autonomous overtaking. In *American Control Conference*, pages 2303–2308, May 2017.

N. A. Nguyen, D. Moser, P. Schrangl, L. del Re, and S. Jones. Autonomous overtaking using stochastic model predictive control. In *11th Asian Control Conference*, pages 1005–1010, Dec 2017.

Athanasios Papoulis. *Probability, Random Variables and Stochastic Processes*. McGraw-Hill, 1965.

P. Petrov and F. Nashahibi. Modeling and nonlinear adaptive control for autonomous vehicle overtaking. *IEEE Transactions on Intelligent Transportation Systems*, 15(4):1643–1656, 2014.

Yadollah Rasekhipour, Amir Khajepour, Shih-Ken Chen, and Bakhtiar Litkouhi. A potential field-based model predictive path-planning controller for autonomous road vehicles. *IEEE Transactions on Intelligent Transportation Systems*, 18:1255 – 1267, 2017.

J.P. Switkes, E.J. Rossetter, and J.C. Gerdes. Experimental validation of the potential field lanekeeping system. *Int J Automot Technol*, 5(2):95–108, 2004.

Christian Wissing, Till Nattermann, Karl-Heinz Glander, Carsten Hass, and Torsten Bertram. Lane change prediction by combining movement and situation based probabilities. *20th IFAC World Congress*, pages 3554–3559, 2017.

Jin Xu, Kui Yang, YiMing Shao, and GongYuan Lu. An experimental study on lateral acceleration of cars indifferent environments in sichuan, southwest china. *Hindawi Publishing Corporation*, pages 1255 – 1267, 2015.

Changxi You, Jianbo Lu, Dimitar Filev, and Panagiotis Tsiotras. Autonomous planning and control for intelligent vehicles in traffic. *IEEE Transactions on Intelligent Transportation Systems (Early Access)*, 2019.

Meihong Zhang, Tingting Zhang, and Qinyu Zhang. An autonomous overtaking maneuver based on relative position information. *2018 IEEE 88th Vehicular Technology Conference*, pages 714–719, 2018.